

## Interspecific comparison of hydrodynamic performance and structural properties among intertidal macroalgae

Michael L. Boller\* and Emily Carrington†

*Department of Biological Sciences, University of Rhode Island, Kingston, RI 02881, USA*

\*Author for correspondence at present address: Hopkins Marine Station, Stanford University, Pacific Grove, CA 93950, USA  
 (e-mail: boller@stanford.edu)

†Present address: Department of Biology, University of Washington, Friday Harbor Laboratories, Friday Harbor, WA 98250, USA

*Accepted 9 March 2007*

### Summary

Macroalgae use flexibility and reconfiguration, i.e. the alteration of shape, size and orientation as water velocity increases, to reduce the hydrodynamic forces imposed in the wave-swept rocky intertidal zone. Quantifying the effects of flexibility on hydrodynamic performance is difficult, however, because the mechanisms of reconfiguration vary with water velocity and the relationship between algal solid mechanics and hydrodynamic performance is poorly understood. In this study, the hydrodynamic performance, morphology and solid mechanics of 10 rocky shore macroalgal species were quantified to evaluate the influences of flexibility and morphology on reconfiguration. Hydrodynamic performance was measured in a flume by direct measurement of changes in size and shape during reconfiguration across a wide range of velocities, material stiffness was quantified with standard materials testing, and structural properties were calculated from

material and morphological data. Hydrodynamic parameters varied significantly among species, indicating variation in the magnitude of reconfiguration and the velocities required for full reconfiguration. Structural properties also varied among species, and were correlated with hydrodynamic performance in some instances. The relationship between hydrodynamic and structural properties is velocity dependent, such that flexibility influences different aspects of reconfiguration at low and high velocities. Groups are identifiable among species based on hydrodynamic and structural properties, suggesting that these properties are useful for addressing functional-form hypotheses and the effects of hydrodynamic disturbance on macroalgal communities.

Key words: biomechanics, beam, modulus, ecology, seaweed.

### Introduction

The flexibility of macroalgae is central to their ability to survive and sometimes dominate the landscape in the harsh hydrodynamic conditions of the wave-swept rocky intertidal zone (Koehl, 1984; Koehl, 1986; Koehl, 1996; Holbrook et al., 1991; Gaylord, 2000; Denny and Gaylord, 2002). The drag imposed on intertidal macroalgae can cause individuals to become dislodged (Dayton, 1973; Paine, 1979; Denny et al., 1985; Carrington, 1990; Dudgeon and Johnson, 1992) or become damaged (Blanchette, 1997). For many species, flexibility results in a reduction in drag *via* reconfiguration, the process by which a macroalga bends in response to drag, changing its shape and size relative to the flow (Vogel, 1984; Vogel, 1989; Vogel, 1994; Koehl, 1986). Thus, traits that improve hydrodynamic performance (e.g. increased reconfiguration and drag reduction) may increase survivorship in the wave-swept rocky shore.

Reconfiguration has been characterized using Vogel's *E*, a

measure of a flexible organism's deviation from the expected relationship between force and velocity seen in rigid organisms (Vogel, 1994). Comparisons of Vogel's *Es* have been made among morphologies and species of macroalgae (Carrington, 1990; Dudgeon and Johnson, 1992; Gaylord et al., 1994; Pratt and Johnson, 2002; Sand-Jensen, 2003; Harder et al., 2004; Boller and Carrington, 2006a). However, this method of characterizing reconfiguration does not address the mechanisms of reconfiguration: changes in size and shape of the organism presented to flow. Boller and Carrington describe a mechanistic approach that separately examines the changes in size and drag coefficient ( $C_D$ , the measure of the influence of shape on drag) of reconfiguring macroalgae (Boller and Carrington, 2006a). For clarity, we will refer to the effects of changing frontal area as 'size' effects and the effects of changing drag coefficient as 'shape' effects, despite the fact that changing size inherently requires changing shape. With this approach, direct measurement of frontal area (the size of

the alga interacting with the flow) and calculation of  $C_D$  across a range of water velocities allows new measures of hydrodynamic performance to be defined. These measures characterize the absolute magnitude of reconfiguration and the water velocity required for full reconfiguration. Boller and Carrington applied this approach to one species (*Chondrus crispus*) (Boller and Carrington, 2006a); one goal of this study is to apply the approach to species spanning a broad range of morphologies.

A second goal of this study is to evaluate the influence of material and structural properties on the hydrodynamic performance of macroalgae. Reconfiguration is a process in which drag may cause a macroalga to bend into a smaller and/or reduced  $C_D$  shape, potentially reducing its risk of dislodgment. Mechanical adaptations that increase the reconfiguration of macroalgae should be beneficial and may be reflected in a correlation between the solid-mechanical characteristics and hydrodynamic performance. Previous studies have examined this relationship in a theoretical and experimental approach in two-dimensional flow (Alben et al., 2002; Alben et al., 2004), have characterized algal solid mechanics but assumed hydrodynamic performance based on environmental exposure (Harder et al., 2006), or used model macroalgae to vary solid mechanical properties (Stewart, 2006). Here, we use an empirical analysis combining the direct quantification of reconfiguration (Boller and Carrington, 2006a) with beam theory to examine how morphology and tissue stiffness influence reconfiguration.

In beam theory (Gere and Timoshenko, 1984; Denny, 1988), the deflection of a beam of a given morphology will increase when the stiffness is decreased. However, beam theory indicates that not just stiffness, but also the cross-

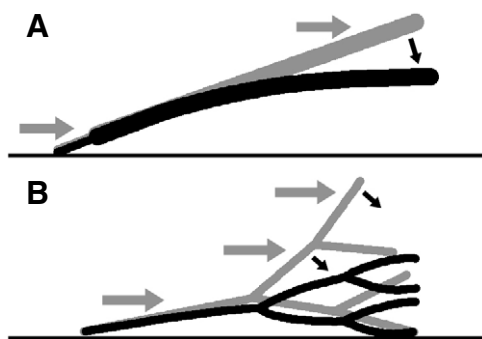


Fig. 1. Conceptual model of macroalgae reconfiguring in flow. Gray and black stick figures represent macroalgae at low and high velocity, respectively. Large gray arrows represent bending force applied by drag. Small black arrows represent the bending moment applied to the beam. (A) Blade-like species, for which force applied along the length of the blade causes deflection and reduction in frontal area. (B) Tree-like species, for which force applied to branches causes bending inward and compression of the branches, reducing the frontal area. Not all forces and moments are drawn.

sectional shape and length of the beam influence bending. Thus, longer beams and less rigid cross-sectional shapes would also be expected to increase bending. This theory has been previously applied to large kelps for which overall flexibility was estimated as 'structural flexibility', an index of the flexibility of a beam that is directly proportional to the length and inversely proportional to stiffness and cross-sectional size of the beam (Denny and Gaylord, 2002).

Beam theory can also be applied to small intertidal macroalgae. For some morphologies (e.g. a long single blade or worm-like alga) the approximation of the macroalga as a beam is straightforward (Fig. 1A). For more complicated shapes, such as tree-like macroalgae, this conceptual model requires modification. The macroalga can be considered a network of connected beams that branches into smaller beams (Fig. 1B). Bending forces are applied to a given beam by drag and physical contact with other branches or the substratum. Together, those forces cause bending of individual beams that results in the overall reduction in frontal area of the macroalga. Because greater flexibility allows greater bending at lower force, the structural flexibility of the beams is hypothesized to be directly proportional to the rate of reconfiguration with increasing velocity. Thus, an *a priori* prediction is that macroalgae with high flexibility require lower velocities to reconfigure.

In addition to influencing the solid mechanics of macroalgae, morphology has been demonstrated to influence hydrodynamic characteristics (e.g. Koehl and Alberte, 1988; Dudgeon and Johnson, 1992; Sand-Jensen, 2003) (see also Carrington, 1990). For example, ruffled kelp blades have higher  $C_D$  than smooth, strap-like blades (Koehl and Alberte, 1988). With respect to reconfiguration, we hypothesize that more complex morphologies (where blades, ruffled blades and branched macroalgae would have increasing complexity) would have a greater capacity for reconfiguration. That is, a branched macroalga with many places to bend can potentially spread out at low velocity (have large area and/or  $C_D$ ) and then reconfigure to a very compact and/or low  $C_D$  morphology at high velocity. Simple morphologies with fewer branch points may have less ability to spread out and thus have less potential to compact and/or change  $C_D$ .

In this study, the effects of morphology and structural properties on hydrodynamic performance were explored by quantifying reconfiguration, material properties and morphology for a range of intertidal macroalgae. Hydrodynamic performance was examined for 10 intertidal macroalgal species with a variety of morphologies by direct measurement of reconfiguration over a wide range of water velocities. The morphology and material stiffness of the macroalgae were quantified, and the relationships among reconfiguration, morphology and material stiffness were examined. Further, the application of these hydrodynamic/solid mechanical data to the identification of functional-form groups was explored.

## Materials and methods

### Study organisms

Ten species of marine macroalgae common and available in the early spring in the rocky intertidal shore of Rhode Island Sound were examined: *Agardhiella subulata* Kraft, *Codium fragile* Har., gametophytic *Chondrus crispus* Stackh., *Fucus vesiculosus* L., *F. distichus* L., *Grateloupia turuturu* Yamada, juvenile *Laminaria saccharina* Lamour, *Mastocarpus stellatus* Guiry, *Petalonia fascia* Kuntze, and *Scytosiphon lomentaria* Link. These species were selected based on their regional availability and range of morphologies. Three to five individuals of each species were haphazardly collected from either Bass Rock (41.40°N, 71.45°W), Black Point (41.39°N, 71.47°W), the University of Rhode Island Bay Campus breakwater (41.49°N, 71.42°W) or Fort Wetherill (41.48°N, 71.36°W) in Rhode Island, USA. Samples were collected by removing a small portion of rock below the holdfast of the alga with a hammer and chisel, preserving the integrity of the holdfast and holdfast-stipe junction. The collection sites varied in community structure such that not all species occurred at each site. To minimize variation within species, all individuals for any given species were collected from a single site. The study was not designed to capture the total variation in hydrodynamic performance across the range of any particular species' morphology, but rather was designed to maximize differences among samples in hydrodynamics, solid mechanics and morphology. Because algae are notoriously plastic in their morphology, it is possible that other samples could deviate from those used here. *Chondrus* gametophytes were identified using a resorcinol test (Garbary and DeWreede, 1988). Samples were maintained in the laboratory in ~17°C seawater for up to three days.

In preparation for hydrodynamic testing, individuals were carefully separated from the rock in the laboratory with a razor blade, and the bottom of the holdfast was shaved to a flat surface. Samples of *Codium* were too large to fit in the experimental apparatus; analyses were conducted on distal branch groups up to 20 cm in height. Algae were attached to the force platform either by the flat bottom of the holdfast or, for *Codium*, by the proximal end of the cut branch using cyanoacrylate glue.

### Hydrodynamic performance

Reconfiguration of each sample was examined using the recirculating seawater flume as per Boller and Carrington (Boller and Carrington, 2006a), with several modifications. Size and drag were quantified at ~0.16 m s<sup>-1</sup> steps up to ~3 m s<sup>-1</sup>. Extremely low velocities (<0.16 m s<sup>-1</sup>) were not examined and are excluded from further references to 'low' velocities. A high-resolution digital camera (C770 Ultra Zoom; Olympus Optical Co., Ltd, Tokyo, Japan) was used to acquire images of the alga projected into the flow. The camera was interfaced to the computer with Camera Controller software (version 1.7.8; Pine Tree Computing, LLC., Olivette, MO, USA). Frontal area (±0.01 cm;  $A_F$ ) was measured from the digital photographs using ImageJ software (version 1.33;

National Institutes of Health, Bethesda, MD, USA).  $A_F$  was normalized by  $A_{rep}$ , the representative area at low reconfiguration, i.e. the size of the alga when realigned such that the stipe is parallel to the flow at  $U \cong 0.16$  m s<sup>-1</sup>.

Drag ( $F_D$ ) at each velocity was measured using a custom force platform capable of measuring three-dimensional force (Boller and Carrington, 2006b). The platform consisted of a plastic post affixed to a three-axis ceramic force transducer (Series109 3D TrackStick; CTS Corp., Elkhart, IN, USA) and three AD623 instrumentation amplifiers (Analog Devices Inc., Norwood, MA, USA) assembled on a four-layer printed circuit board designed using ExpressPCB software (www.ExpressPCB.com). The amplified analog force was converted to a digital signal (DAS16-AO; Measurement Computing Corp., Middleboro, MA, USA) and recorded by a PC at a rate of 100 Hz for 10 s using Softwire software (version 3.1; Measurement Computing Corp.). The force platform was calibrated for each axis by hanging weights from a string glued to the surface of the post when the platform was held on its side. During hydrodynamic tests, the vector average of the three axes was calculated at each sample interval, and  $F_D$  at each specific velocity was calculated as the average magnitude of the 1000 vectors (±0.01 N).

Drag coefficient ( $C_D$ ) was calculated at each velocity as:

$$C_D \equiv \frac{2F_D}{\rho U^2 A_F}, \quad (1)$$

where  $\rho$  is the density of the fluid (1025 kg m<sup>-3</sup>),  $U$  is the velocity of the fluid relative to the organism in m s<sup>-1</sup>, and  $A_F$  is the frontal area at  $U$ .

Hydrodynamic performance data were pooled within each species, and the normalized area as a function of velocity ( $a_U$ ) was described as an exponential decay function:

$$a_U = a_\infty + a_R e^{-U/\beta_a}, \quad (2)$$

where  $a_\infty$  is the minimum normalized area of the alga (a measure of maximum reconfiguration),  $a_R$  is a coefficient describing the magnitude of area reduced because of reconfiguration, and  $\beta_a$  is the reconfiguration coefficient of area, a term that describes the steepness of the decay function. The drag coefficient as a function of water velocity ( $C_U$ ) was also described as an exponential decay process:

$$C_U = C_\infty + C_R e^{-U/\beta_C}, \quad (3)$$

where  $C_\infty$  is the minimum  $C_D$  ( $C_D$  at maximum reconfiguration),  $C_R$  is a coefficient describing the magnitude of the reduction of  $C_D$  because of reconfiguration, and  $\beta_C$  is the reconfiguration coefficient for  $C_D$ . Parameters for both functions were estimated for each species using TableCurve2D software (version 4.07; Systat Software Inc., Point Richmond, CA, USA). Large sample normal approximate confidence intervals, an approximation of 99% confidence intervals, were calculated by multiplying the standard error reported by TableCurve2D by ±2.5758 [the value of the 99th percentile of

a normal frequency distribution of  $\infty$  samples (Underwood, 1997)]. Significant differences among species and pairwise comparisons were defined by the lack of overlap of confidence intervals.

#### Morphology and solid mechanics

The morphology of each species was quantified by measuring five features. Each sample was first sandwiched between two acrylic sheets and photographed from above with the digital camera. Planform area ( $\pm 0.01 \text{ cm}^2$ ) was measured from the photograph with ImageJ. Branch lengths ( $\pm 0.01 \text{ mm}$ ) were measured in ImageJ from the tip of the alga to the lowest branching point above the stipe (for blade-like species, a branch is equivalent to a blade). Branch width and thickness were measured either with digital calipers ( $\pm 0.01 \text{ mm}$ ) or with ImageJ using an image of the cross-section of a branch. Cross-sectional area was then calculated assuming an ellipse for rounded cross-sections, a rectangle for very flat cross-sections, or directly measured with ImageJ for complexly shaped cross-sections. For hollow species (*Scytosiphon* and *Agardhiella*), the thickness of one layer of the tissue was used as the measure of branch diameter, and the thickness multiplied by the circumference was used as the measure of cross-sectional area of the branch.

Standard materials testing was performed as per Carrington et al. (Carrington et al., 2001) on samples from each alga using a computer-interfaced tensometer (model 5565; Instron Corp., Canton, MA, USA) equipped with a noncontacting video extensometer (model 2663; Instron Corp.). For most species, 3 cm-long samples were dissected from undamaged and non-reproductive branches in the central portion of the alga. For blade-like species, rectangular samples ( $1 \times 3 \text{ cm}$ ,  $W \times L$ ) were cut from the blade using two single-edge razors affixed to a 1 cm-wide aluminum block. Stipe and apical tissue was not characterized mechanically. The ends of each sample were held by a pair of pneumatic grips lined with fine sandpaper at a pressure of  $4 \text{ kg cm}^{-2}$ . Two silver-paint dots, applied approximately 5 mm apart to the center of the sample, defined the length of the test region. The samples were periodically wetted with seawater to prevent desiccation. Force ( $\pm 0.001 \text{ N}$ ) was measured with a 50-N load cell at an extension rate of  $50 \text{ mm min}^{-1}$  while the extensometer simultaneously measured extension ( $\pm 0.005 \text{ mm}$ ) as the distance between the two dots. Whereas material properties may be strain-rate-dependent, algal tissues have been shown to have relatively constant properties across large ranges of strain rate (Gaylord et al., 2001), justifying the use of a single strain rate. Stress ( $\sigma$ ) was calculated as the force divided by the initial cross-sectional area of the sample. Strain ( $\epsilon$ ) was calculated from the extension using the formula  $(l-l_0)/l_0$ , where  $l_0$  was the initial length of the test region and  $l$  was the length measured by the extensometer. The modulus ( $E$ , not to be confused with Vogel's  $E$ ), or material stiffness, was calculated as the slope of the steepest linear portion of the stress-strain curve. An index of the structural flexibility was calculated for each individual macroalga as  $L^3/ED^4$ , where  $L$  was the average branch length

and  $D$  was the average minimum dimension of the branch cross-sections or the average thickness of the tissue for hollow species (Denny and Gaylord, 2002).

For statistical analysis, structural flexibility was normalized by log transformation to remove skew (Underwood, 1997);  $E$  was untransformed. One-way analyses of variance (ANOVAs) were performed on each structural property using Systat software (version 11.0; Systat Software Inc.). In addition, Tukey's pairwise comparisons were performed to examine relationships among species.

#### Correlation of hydrodynamic performance with solid mechanics

The relationships between hydrodynamic performance and solid mechanical properties were examined among species by calculating four hydrodynamic performance measures derived from  $a_U$  and  $C_D$  functions for each species (Boller and Carrington, 2006a). To compare the rate of reconfiguration with increasing water velocity among species, the critical velocity of area reconfiguration ( $U_{\text{crit,a}}$ ) was defined as the velocity at which  $a_U$  came within 5% of the minimum value ( $a_\infty$ ). The critical velocity of  $C_D$  reconfiguration ( $U_{\text{crit,C}}$ ) was defined as the velocity at which  $C_D$  came within 5% of the minimum value ( $C_\infty$ ). In addition, two indexes were calculated to compare reconfiguration at low ( $0.5 \text{ m s}^{-1}$ ) and high ( $3.0 \text{ m s}^{-1}$ ) water velocities. 'Compaction' was defined as the proportion of area reconfiguration achieved at a given velocity and was calculated as  $1-a_U$ , where  $a_U$  was the solution of Eqn 2 at either  $0.5$  or  $3 \text{ m s}^{-1}$ . Drag coefficients were also calculated for each species at each velocity by solving Eqn 3. The dependence of these four hydrodynamic performance measures on each of two solid mechanical properties (log-transformed structural flexibility and modulus) was evaluated using linear regression analysis (Systat version 11.0).

## Results

### Hydrodynamic performance

Hydrodynamic performance varied among species for both normalized area and drag coefficient (Fig. 2). Normalized frontal area was described well by Eqn 2 for all species (all  $P < 0.01$ ,  $R^2 = 0.80$  to  $0.98$ ; Table 1, Fig. 3A). Lack of overlap of confidence intervals for  $a_\infty$ ,  $a_R$  and  $\beta_a$  indicated significant differences among species for all parameters (Table 1).  $U_{\text{crit,a}}$  ranged from  $0.92$  to  $4.21 \text{ m s}^{-1}$  among species (Table 1). Among the curves of Fig. 3A, three general patterns can be identified: two species (*Mastocarpus* and *Chondrus*) exhibited more resistance to reconfiguration with increasing water velocity (i.e. required higher velocity to reconfigure,  $U_{\text{crit,a}}$ ) and moderate levels of total reconfiguration (i.e.  $a_\infty$ ). *F. distichus*, *F. vesiculosus*, *Codium*, *Agardhiella* and *Scytosiphon* had relatively less resistance to reconfiguration, but varying levels of total reconfiguration. Three species (*Laminaria*, *Petalonia* and *Grateloupia*) displayed the largest resistance to reconfiguration and high levels of total reconfiguration (low  $a_\infty$ ).

Table 1. Normalized area model parameters for 10 intertidal algae

Species	$a_{\infty}$	$a_R$	$\beta_a$	$R^2$	$U_{crit,a}$
<i>Grateloupa</i>	0.26±0.02 <sup>a</sup>	0.90±0.04 <sup>c</sup>	0.71±0.07 <sup>d</sup>	0.97	3.03
<i>Laminaria</i>	0.32±0.06 <sup>a,b,c</sup>	0.74±0.12 <sup>a,b,c</sup>	0.67±0.27 <sup>b,c,d,e</sup>	0.81	2.59
<i>Petalonia</i>	0.28±0.05 <sup>a,b</sup>	0.86±0.09 <sup>b,c</sup>	0.72±0.20 <sup>c,d,e</sup>	0.93	2.99
<i>Agardhiella</i>	0.35±0.03 <sup>b,c</sup>	0.91±0.13 <sup>c</sup>	0.38±0.08 <sup>a,b</sup>	0.92	1.50
<i>Scytosiphon</i>	0.34±0.03 <sup>b,c</sup>	1.00±0.16 <sup>c</sup>	0.37±0.08 <sup>a,b</sup>	0.90	1.50
<i>Chondrus</i>	0.39±0.03 <sup>c</sup>	0.71±0.03 <sup>a</sup>	0.77±0.10 <sup>d,e</sup>	0.98	2.76
<i>Codium</i>	0.46±0.02 <sup>d,e</sup>	0.75±0.12 <sup>a,b,c</sup>	0.38±0.09 <sup>a,b</sup>	0.91	1.34
<i>F. distichus</i>	0.40±0.03 <sup>c,d</sup>	0.76±0.11 <sup>a,b,c</sup>	0.48±0.12 <sup>a,b,c</sup>	0.80	1.76
<i>F. vesiculosus</i>	0.51±0.04 <sup>e</sup>	0.88±0.29 <sup>a,b,c</sup>	0.26±0.10 <sup>a</sup>	0.80	0.92
<i>Mastocarpus</i>	0.35±0.07 <sup>a,b,c</sup>	0.71±0.06 <sup>a,b</sup>	1.14±0.30 <sup>e</sup>	0.88	4.21

Values are means ± large-sample, normal approximate confidence intervals from Eqn 2.

The minimum normalized area ( $a_{\infty}$ ) and the area reduced during reconfiguration ( $a_R$ ) are unitless, whereas the reconfiguration coefficient of area ( $\beta_a$ ) and the critical velocity of area reconfiguration ( $U_{crit,a}$ ) have units of  $m s^{-1}$ . Superscript letters next to values denote groups defined by the overlap of confidence intervals.

Drag coefficients were more variable than normalized frontal area within a species (Fig. 2) but were still described well by Eqn 3 (all  $P < 0.01$ ,  $R^2 = 0.59$  to 0.83; Table 2, Fig. 3B). Lack of overlap of confidence intervals indicated significant

differences among species.  $U_{crit,C}$  varied from 0.88 to  $1.90 m s^{-1}$  among species (Table 2), but less variation in  $C_D$  reconfiguration was evident, such that groups were not identifiable as in normalized area (Fig. 3B).

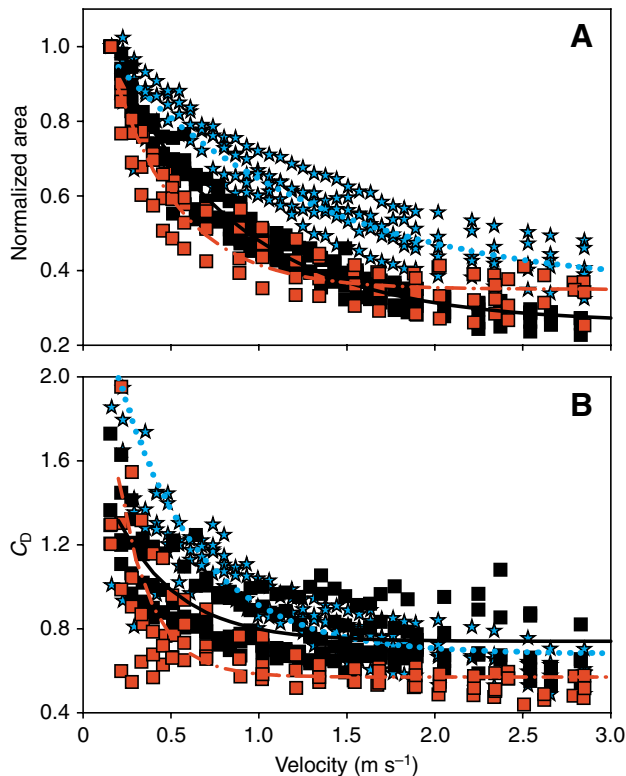


Fig. 2. Normalized area and drag coefficient as functions of velocity for three representative species. (A) Each line is  $a_U$ , the curve fit of Eqn 2 to pooled data from 3–5 individuals of each species. (B) Each line is  $C_U$ , the curve fit of Eqn 3 to pooled data from 3–5 individuals of each species. Species labeled as: *Grateloupa* (■, —), *Agardhiella* (■, - - -) and *Mastocarpus* (★, · · ·). Form is denoted by the color of the line, where black=blade-like, red=whip-like and blue=tree-like.

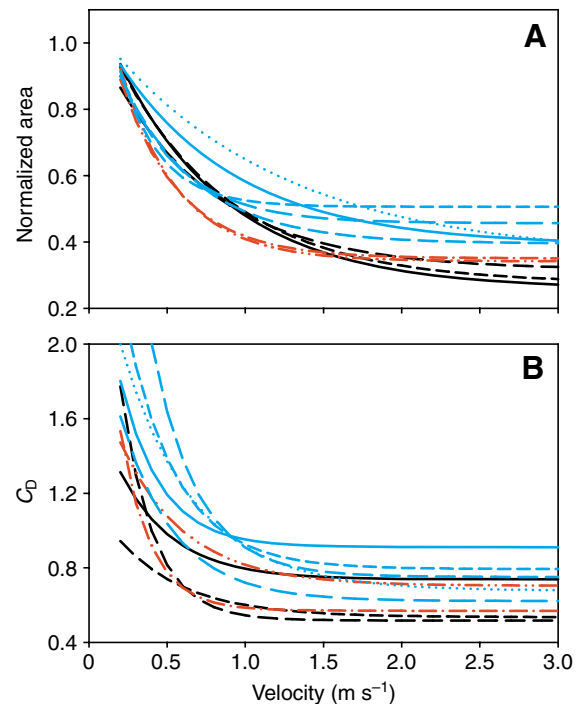


Fig. 3. Summary curves of normalized area and drag coefficient as functions of velocity for 10 species of rocky intertidal macroalgae. (A) Each line is  $a_U$ , the curve fit of Eqn 2 to pooled data from 3–5 individuals of each species. (B) Each line is  $C_U$ , the curve fit of Eqn 3 to pooled data from 3–5 individuals of each species. Species labeled as: *Grateloupa* (—), *Laminaria* (---), *Petalonia* (- - -), *Agardhiella* (- · · -), *Scytosiphon* (- · · · -), *Chondrus* (— — —), *Codium* (— — —), *F. distichus* (- - -), *F. vesiculosus* (- - -) and *Mastocarpus* (· · ·). Form is denoted by the color of the line, where black=blade-like, red=whip-like and blue=tree-like.

Table 2. Drag coefficient model parameters for 10 intertidal algae

Species	$C_\infty$	$C_R$	$\beta_C$	$R^2$	$U_{crit,C}$
<i>Grateloupia</i>	0.74±0.04 <sup>c</sup>	1.02±0.29 <sup>a,b</sup>	0.35±0.13 <sup>a,b</sup>	0.61	1.16
<i>Laminaria</i>	0.52±0.10 <sup>a,b</sup>	3.28±1.50 <sup>d,e</sup>	0.21±0.09 <sup>a</sup>	0.66	1.01
<i>Petalonia</i>	0.54±0.06 <sup>a</sup>	0.65±0.25 <sup>a</sup>	0.43±0.26 <sup>a,b</sup>	0.63	1.38
<i>Agardhiella</i>	0.57±0.07 <sup>a,b,c</sup>	2.71±1.10 <sup>c,d,e</sup>	0.19±0.07 <sup>a</sup>	0.74	0.88
<i>Scytosiphon</i>	0.70±0.09 <sup>b,c</sup>	1.24±0.50 <sup>a,b,c</sup>	0.42±0.23 <sup>a,b</sup>	0.60	1.48
<i>Chondrus</i>	0.91±0.08 <sup>d</sup>	1.92±0.74 <sup>b,c,d</sup>	0.26±0.11 <sup>a</sup>	0.73	0.98
<i>Codium</i>	0.62±0.14 <sup>a,b,c</sup>	1.77±0.79 <sup>b,c,d</sup>	0.35±0.21 <sup>a,b</sup>	0.59	1.40
<i>F. distichus</i>	0.75±0.14 <sup>b,c,d</sup>	4.99±1.22 <sup>e</sup>	0.29±0.08 <sup>a,b</sup>	0.76	1.42
<i>F. vesiculosus</i>	0.79±0.16 <sup>c,d</sup>	2.69±1.04 <sup>c,d</sup>	0.33±0.15 <sup>a,b</sup>	0.77	1.39
<i>Mastocarpus</i>	0.68±0.06 <sup>b,c</sup>	2.03±0.29 <sup>c,d</sup>	0.46±0.10 <sup>b</sup>	0.83	1.90

Values are means ± large-sample, normal approximate confidence intervals from Eqn 3.

The minimum  $C_D$  ( $C_\infty$ ) and the  $C_D$  reduced during reconfiguration ( $C_R$ ) are unitless, whereas the reconfiguration coefficient of  $C_D$  ( $\beta_C$ ) and the critical velocity of  $C_D$  reconfiguration ( $U_{crit,C}$ ) have units of  $m\ s^{-1}$ . Superscript letters next to values denote groups defined by the overlap of confidence intervals.

### Morphology and solid mechanics

Planform areas, ranging from 8.03 to 172.62  $cm^2$ , were large and variable compared with representative areas, which ranged from 3.99 to 23.94  $cm^2$  (Table 3). Average height (range=5.97–23.51 cm), branch length (range=3.66–18.61 cm) and branch diameters (range=0.06–4.55 mm), the later two used to calculate structural flexibility, are reported in Table 3.

Significant differences were evident among structural properties (Table 4).  $E$  ranged from 0.77 to 25.77  $MN\ m^{-2}$  and varied significantly among species (Table 5). Structural flexibility ranged from  $1.18 \times 10^7$  to  $6.25 \times 10^{12}$   $m\ MN^{-1}$  and varied significantly (Table 5).

### Correlation of hydrodynamic performance to solid mechanics

Hydrodynamic performance correlated significantly with solid mechanical properties in some, but not all, instances. No significant relationships were observed between the critical velocities ( $U_{crit,a}$  and  $U_{crit,C}$ ) and solid mechanical properties (all regressions  $P > 0.05$ , Fig. 4). Compaction and drag coefficient correlated significantly with solid mechanical properties at some velocities (Figs 5, 6). At low velocity

(0.5  $m\ s^{-1}$ ), compaction decreased with modulus (slope=−0.005,  $R^2=0.39$ ,  $P=0.05$ ; Fig. 5B) but had no relationship with structural flexibility ( $P > 0.05$ ; Fig. 5A). At high velocity (3  $m\ s^{-1}$ ), compaction increased with structural flexibility (slope=0.029,  $R^2=0.73$ ,  $P < 0.01$ ; Fig. 5C) but was not correlated with stiffness (Fig. 5D;  $P > 0.05$ ). For drag coefficient, significant correlations were evident for both structural flexibility (slope=−0.093,  $R^2=0.47$ ,  $P=0.03$ ; Fig. 6A) and stiffness (slope=0.026,  $R^2=0.50$ ,  $P=0.02$ ; Fig. 6B) at low water velocity (0.5  $m\ s^{-1}$ ). At high water velocity, no significant correlations between  $C_D$  and structural properties were evident ( $P > 0.05$ ; Fig. 6C,D).

## Discussion

### Hydrodynamic performance

The hydrodynamic performances of all species are described well by the exponential decay functions of the reconfiguration drag model (Boller and Carrington, 2006a), despite the large variation in material and morphological properties among species. Variation in reconfiguration among species may have

Table 3. Morphological characteristics for 10 intertidal macroalgae examined in this study

Species	$N$	Planform area ( $cm^2$ )	Representative area ( $cm^2$ )	Height (cm)	Branch diameter (mm)	Branch length (cm)
<i>Grateloupia</i>	5	172.62±35.35	23.56±3.57	23.51±3.96	0.25±0.04	17.99±5.11
<i>Laminaria</i>	3	85.06±46.50	11.13±2.05	16.23±4.37	0.14±0.05	16.23±4.37
<i>Petalonia</i>	4	60.66±17.42	5.53±0.41	11.16±2.44	0.06±0.01	7.04±1.26
<i>Agardhiella</i>	4	75.86±33.50	9.38±2.93	11.67±2.59	0.43±0.01	11.63±2.58
<i>Scytosiphon</i>	4	53.67±17.08	6.37±1.33	20.82±2.25	0.11±0.02	18.61±2.25
<i>Codium</i>	4	121.56±43.91	17.42±2.37	17.49±2.27	4.55±0.38	14.25±1.30
<i>Chondrus</i>	4	35.96±17.90	16.99±10.74	8.42±1.52	0.36±0.06	5.52±1.07
<i>F. distichus</i>	5	137.62±122.08	23.94±14.97	11.84±1.34	0.71±0.06	6.84±1.37
<i>F. vesiculosus</i>	4	81.32±12.95	16.22±4.84	14.61±2.41	0.97±0.09	10.16±0.93
<i>Mastocarpus</i>	5	8.03±3.65	3.99±2.22	5.97±0.53	0.36±0.05	3.66±0.44

Values are means ± s.d.

Table 4. Summary of one-way ANOVA results for structural properties

Source	d.f.	Mean square	F ratio	P value
Modulus ( $E$ )				
Species	9	282.02	17.57	<0.01
Error	31	16.05		
Log structural flexibility				
Species	9	18.47	183.37	<0.01
Error	31	0.10		

ecological importance at moderate velocities. For example, individuals exhibiting less reconfiguration will be exposed to more force but may have competitive advantage for space and light competition and less self-shading. At high velocities, however, the results suggest that macroalgae act as rigid objects, with drag increasing with the square of velocity. At these velocities, variation in reconfiguration will no longer matter. Quantification of drag coefficients for rigid and flexible intertidal organisms at high velocities is needed to fully understand the hydrodynamic forces of the wave-swept rocky intertidal zone.

It should be noted that this measure of the capacity of area reconfiguration ( $a_{\infty}$ ) is an underestimate of the total ability of a species to reconfigure because the extremely low velocity changes that occur as the macroalga realigns are not included. That is, at still water, the projected area would be the side of the upright macroalga (approximately the planform area). After realignment, the projected area is effectively the top of the macroalga (the representative area).  $a_{\infty}$  characterizes the degree of reconfiguration starting when the macroalga is the size of

Table 5. Modulus ( $E$ ) and structural flexibility of 10 rocky intertidal species examined in this study

Species	$N$	$E$ (MN m <sup>-2</sup> )	Structural flexibility (m MN <sup>-1</sup> )
<i>Grateloupia</i>	5	5.33±0.82 <sup>a,b</sup>	3.66±2.52×10 <sup>11</sup> e
<i>Laminaria</i>	3	9.95±3.35 <sup>b,c</sup>	12.0±3.49×10 <sup>11</sup> e,f
<i>Petalonia</i>	3	7.25±1.41 <sup>a,b</sup>	6.25±4.49×10 <sup>12</sup> f
<i>Agardhiella</i>	4	3.19±0.67 <sup>a,b</sup>	15.4±9.01×10 <sup>9</sup> d
<i>Scytosiphon</i>	4	11.64±1.79 <sup>b,c</sup>	4.11±2.85×10 <sup>12</sup> f
<i>Codium</i>	4	0.77±0.47 <sup>a</sup>	11.8±6.99×10 <sup>6</sup> a
<i>Chondrus</i>	4	19.20±3.21 <sup>c,d</sup>	5.53±1.75×10 <sup>8</sup> c
<i>F. distichus</i>	5	19.27±5.46 <sup>c,d</sup>	8.81±6.66×10 <sup>7</sup> b
<i>F. vesiculosus</i>	4	11.95±1.67 <sup>b,c</sup>	11.2±6.44×10 <sup>7</sup> b,c
<i>Mastocarpus</i>	5	25.77±8.63 <sup>d</sup>	1.55±1.05×10 <sup>8</sup> b,c

Values are species means ± s.d. Superscript letters next to values denote groups defined by Tukey's pairwise comparisons.

the representative area. Further, the variation in planform areas was much larger than in representative areas, indicating that extremely low velocity realignment narrowed the effective range of algal sizes in this study.

The flexibility and reconfiguration of macroalgae has been said to decouple shape from hydrodynamic force generation (Denny and Gaylord, 2002). Here, where the effects of macroalga shape and size are separated, the mollifying effect of flexibility is also evident. Comparison of low (more variable) and high (less variable) velocity  $C_D$  suggests that drag coefficients converge at high velocities as reconfiguration conforms algae to a compacted shape (Fig. 3B). Further, all of the  $C_{\infty}$  reported here are similar to those of bluff bodies (i.e.

non-streamlined, rigid objects with  $C_D > 0.5$ ) (Hoerner, 1965), suggesting that none of the macroalgae have a truly hydrodynamically superior shape despite the range of still-water morphologies. Thus, in terms of the influence of shape on drag generation, the different morphologies are hydrodynamically similar, as was found in a previous study (Carrington, 1990). This moderating effect of reconfiguration on the hydrodynamics of flexible macroalgae has probably enabled the evolution of the wide variety of morphologies seen even in the harsh wave-swept rocky intertidal zone.

In as much as these data are representative of the species in general, comparisons can be made regarding the relative contributions of changes in size and  $C_D$  among species. Many species have higher  $U_{crit,a}$  than  $U_{crit,C}$ , indicating that size continues to change after  $C_D$  has become constant (Fig. 7). Thus, for these species, reconfiguration at intermediate velocities is dominated by changes in

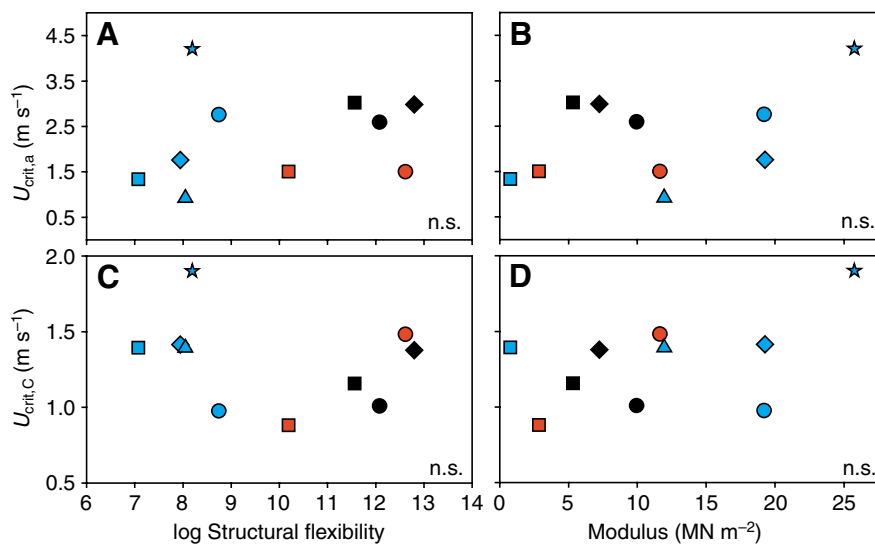


Fig. 4.  $U_{crit,a}$  and  $U_{crit,C}$  versus the structural flexibility and modulus. (A)  $U_{crit,a}$  versus structural flexibility. (B)  $U_{crit,a}$  versus modulus. (C)  $U_{crit,C}$  versus structural flexibility. (D)  $U_{crit,C}$  versus modulus. No linear regressions were significant ( $P > 0.05$ ). Species labeled as: *Grateloupia* (■), *Laminaria* (●), *Petalonia* (◆), *Agardhiella* (■), *Scytosiphon* (●), *Codium* (■), *Chondrus* (●), *F. distichus* (◆), *F. vesiculosus* (▲) and *Mastocarpus* (★). Form is denoted by the color of the line, where black=blade-like, red=whip-like and blue=tree-like.

projected area, not changes in  $C_D$ , suggesting that changes in the overall size of the macroalgae presented to the flow is more important than the shape. However, some species (*Codium*, *F. distichus*, *F. vesiculosus* and *Scytosiphon*) have similar, low  $U_{crit,C}$  and  $U_{crit,a}$ , suggesting that they experience size and shape effects across similar ranges in velocity. Further, these similar

$U_{crit}$  values are probably because of lower  $U_{crit,a}$  values, suggesting these species reach their maximum potential reconfiguration across smaller changes in velocity.

The dynamic nature of reconfiguration is evident in these results. The relative magnitudes of parameters among some species change as water velocity increases, suggesting conclusions drawn from low-velocity studies may not be appropriate at high velocities (Carrington, 1990; Vogel, 1994; Bell, 1999; Denny and Gaylord, 2002; Boller and Carrington, 2006a). For area reconfiguration, *F. distichus* and *F. vesiculosus* have lower normalized area than *Chondrus* and *Mastocarpus* at  $0.75 \text{ m s}^{-1}$  (Fig. 3A), but this relationship is overturned at  $3 \text{ m s}^{-1}$ . However, the reconfiguration drag model describes these velocity-dependent differences where frontal area and  $C_D$  approach asymptotes. Only *Mastocarpus* and *Grateloupia* were predicted to continue to reduce in size beyond the range of this study, suggesting that for the majority of species extrapolation beyond  $3 \text{ m s}^{-1}$  is possible. A high-velocity test of the model is needed to justify this extrapolation.

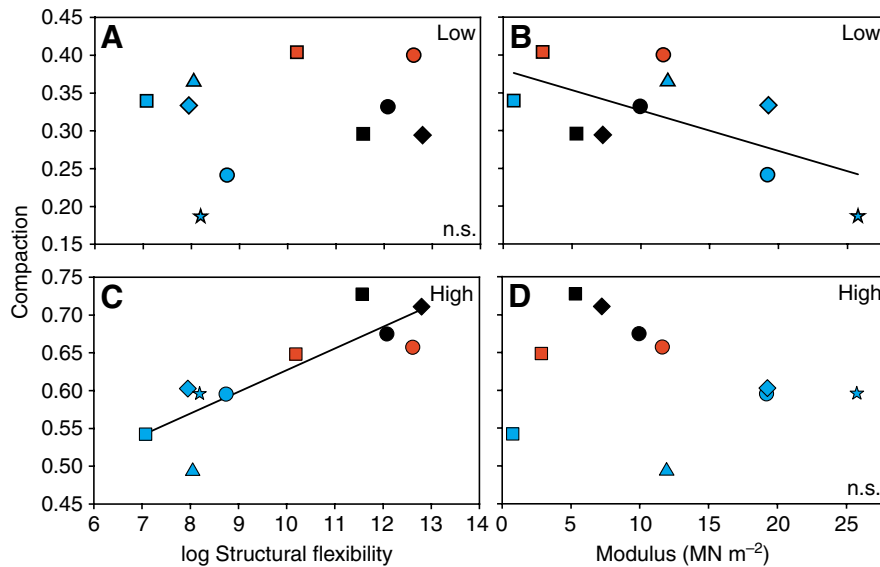


Fig. 5. Compaction, the proportion of area lost because of reconfiguration, versus structural properties. (A,B) Low velocity ( $0.5 \text{ m s}^{-1}$ ). (C,D) High velocity ( $3.0 \text{ m s}^{-1}$ ). Regression of low velocity compaction to modulus (slope= $-0.005$ ,  $R^2=0.39$ ,  $P=0.05$ ) and high velocity compaction to log structural flexibility were significant (slope= $0.029$ ,  $R^2=0.73$ ,  $P<0.01$ ). Other regressions were not significant ( $P>0.05$ ). Species labeled as per Fig. 4.

### Structural properties

Although material stiffness varied among species, all species in the study have low stiffness compared with other, non-algal biological materials (Wainwright et al., 1976; Denny, 1988). The moduli reported in this study ( $0.77$  to  $25.77 \text{ MN m}^{-2}$ , Table 5) are similar to the range reported elsewhere for macroalgae ( $1$  to  $100 \text{ MN m}^{-2}$ ) (Dudgeon and Johnson, 1992; Carrington et al., 2001; Hale, 2001; Denny and Gaylord, 2002). Of note is the exceptionally low modulus of *Codium* ( $0.77 \text{ MN m}^{-2}$ ) that is probably because of its siphonous growth form (Graham and Wilcox, 2000). *Codium* has multiple siphons that are highly interwoven to form the thallus. This design probably allows for movement of siphons relative to each other and thus a lower modulus. Other species in the study (*Chondrus*, *Mastocarpus* and *Agardhiella*) are pseudoparenchymatous [filaments that coalesce to form macroscopic thalli (Graham and Wilcox, 2000)], and this more integrated construction may yield higher moduli.

Among the species, lower modulus (stiffness) does not always confer greater

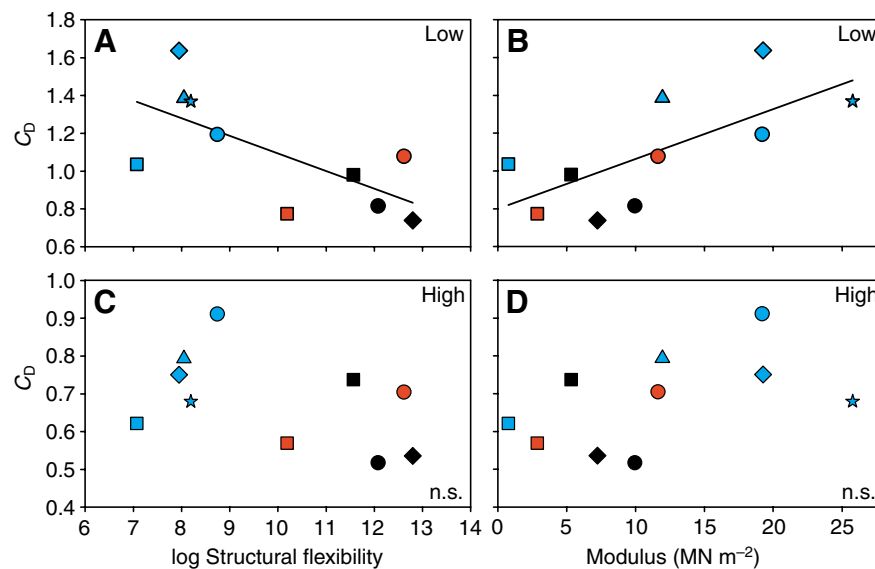


Fig. 6. Drag coefficient versus structural properties. (A,B) Low velocity ( $0.5 \text{ m s}^{-1}$ ). (C,D) High velocity ( $3.0 \text{ m s}^{-1}$ ). Linear regressions of  $C_D$  to log-transformed structural flexibility (slope= $-0.093$ ,  $R^2=0.47$ ,  $P=0.03$ ) and  $C_D$  to modulus (slope= $0.026$ ,  $R^2=0.50$ ,  $P=0.02$ ) were significant at low velocity. Neither relationship was significant at high velocity ( $P>0.05$ ). Species labeled as per Fig. 4.



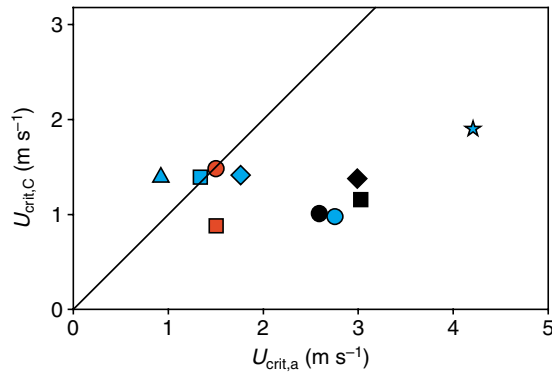


Fig. 7. The critical velocities of normalized area ( $U_{crit,a}$ ), the velocity at which area reaches within 5% of the minimum area, versus the critical velocity of drag coefficient ( $U_{crit,C}$ ), the velocity at which  $C_D$  reaches within 5% of the minimum  $C_D$ . The line is unity. Note that most species fall below the line, indicating that  $C_D$  asymptotes at a lower velocity than normalized area for those species. Species labeled as per Fig. 4.

structural flexibility. *Codium* has the lowest flexibility because of its extremely large branch diameter, despite its order of magnitude lower modulus and long branches. Other tree-like species have moderately thick and short branches and generally higher stiffness, which also results in low flexibility. High flexibility is seen among blade- and whip-like species, because of their long branch length and small branch diameters.

#### *Do structural properties influence hydrodynamic performance?*

Stewart used flexural stiffness (Stewart, 2006), the product of the modulus and the second moment of area (a measure of cross-sectional shape relative to the applied force), to examine the relationship between hydrodynamic performance and solid mechanics for morphologically identical model seaweeds. In that study, stiffness significantly influenced drag generation, but only for the most flexible models that had an order of magnitude lower modulus. Conversely, Dudgeon and Johnson observed greater reconfiguration in a stiff species (*Mastocarpus*) than in a more flexible species (*Chondrus*) (Dudgeon and Johnson, 1992). Harder et al. observed a correlation between tissue stiffness and exposure (Harder et al., 2006), suggesting that lower stiffness bestows greater reconfiguration and survival.

In this study, we hypothesized that higher structural flexibility would result in higher rates of reconfiguration and subsequently require lower velocities to fully reconfigure (lower  $U_{crit,a}$  and  $U_{crit,C}$ ). However, this pattern was not observed (Fig. 4). Structural flexibility was positively

correlated with compaction at high velocity and negatively related to  $C_D$  at low velocity. This pattern may be because of a correlation between structural flexibility and morphology, where blade-like species had higher compaction than more complex species, as discussed below.

More complex morphologies were hypothesized to have greater capacity for reconfiguration and thus have lower  $a_\infty$ . Results suggest the opposite is true: blade-like species had the lowest  $a_\infty$  among the species studies. This pattern may be because of the cross-sectional size and number of an alga's branches when bent and pushed together. That is, the absolute minimum size a blade-like macroalga can achieve through reconfiguration may be less than the minimum size of a dichotomously branching macroalga simply because the blade has less tissue and can compact tightly because of its simple shape.

The application of beam theory requires some simplifying assumptions that may be inappropriate for intertidal macroalgae. For example, branches are assumed to bend as cantilevers. However, the torsion of branches may be important for the compaction of blades. Thus, variation in torsion modulus among macroalgal species (Harder et al., 2006) may influence reconfiguration. Further, tissue stiffness in compression and tension may differ and influence bending of branches (Koehl and Wainwright, 1977; Gaylord and Denny, 1997). A more complex structural model of macroalgal bending may clarify the relationship between hydrodynamic performance and structural properties. Alternatively, an empirical test of whole thallus structural mechanics may provide the data to correlate solid mechanical and hydrodynamic performances.

#### *Functional-form groups*

The characterization of hydrodynamic performance of the various algal morphologies found in the rocky intertidal zone may be useful for defining functional-form groups based on resistance to hydrodynamic disturbance (Padilla and Allen, 2000). This functional-form approach to addressing wave disturbance may allow for better understanding of community and landscape ecology of the rocky shore. Larger sample sizes incorporating the range of morphological variation within a species are needed to fully test this application of the data, but some trends can be pointed out from our results (Table 6).

Blade-like species (*Laminaria*, *Petalonia* and *Grateloupia*) are more flexible and achieved the highest degree of size reconfiguration (low  $a_\infty$ ) and generally low  $C_\infty$ . However, blades required high velocities to accomplish reconfiguration (high  $U_{crit,a}$ ). Together, these qualities suggest that blade-like species have great capacity to reduce the effects of drag, as

Table 6. Summary of hydrodynamic characteristics of forms

Form	Area reconfiguration	$C_D$ reconfiguration
Blade	Most compressible, high critical velocity	Most streamlined, variable critical velocity
Whip	Intermediately compressible, intermediate critical velocity	Intermediately streamlined, variable critical velocity
Tree	Least compressible, variable critical velocity	Least streamlined, variable critical velocity

found in a previous study (Carrington, 1990). Tree-like species (*Chondrus*, *F. distichus*, *F. vesiculosus*, *Codium* and *Mastocarpus*) are generally stiffer but variable in the rate of reconfiguration; they are generally less reconfigurable in size (high  $a_\infty$ ) and have relatively high drag coefficient (high  $C_\infty$ ), suggesting that this morphology is least effective at reducing the stress of intertidal flows. The variation in hydrodynamic performance observed among these species probably reflects the morphological variation in this loosely termed group. The performances of whip-like species (*Agardhiella* and *Scytosiphon*) are intermediate to blade- and tree-like species.

### Conclusions

The reconfiguration drag model successfully characterizes the hydrodynamic performance of morphologically distinct intertidal macroalgae. Hydrodynamic, structural and morphological properties all vary significantly among species. Structural properties are correlated with some aspects of hydrodynamic performance, but those correlations between performance and structural properties are velocity dependent. Different mechanisms (size *versus* shape change) are responsible for reconfiguration at different velocities. Functional-form groups based on performance and structural properties are discernible, suggesting that these physical measurements of the organisms' interactions with the environment may be useful for understanding the ecology of these biomechanically complex organisms.

### List of abbreviations and symbols

Symbol		Equation where first used
$a_\infty$	Minimum normalized area	2
$a_R$	Normalized area reduced because of reconfiguration	2
$a_U$	Normalized area as a function of velocity	2
$A_F$	Frontal area	1
$A_{rep}$	Representative area at low reconfiguration	–
$\beta_a$	Reconfiguration coefficient of normalized area	2
$\beta_C$	Reconfiguration coefficient of the drag coefficient	3
$C_D$	Drag coefficient	1
$C_\infty$	Minimum drag coefficient	3
$C_R$	Drag coefficient reduced because of reconfiguration	3
$C_U$	Drag coefficient as a function of velocity	3
$D$	Branch diameter	–
$E$	Modulus	–
$\epsilon$	Strain	–
$F_D$	Drag	1
$l$	Extension	–

$l_0$	Initial length of sample in tensile tests	–
$L$	Branch length	–
$\rho$	Fluid density	1
$\sigma$	Stress	–
$U$	Velocity of the fluid relative to the organism	1
$U_{crit,a}$	Critical velocity of area reconfiguration	–
$U_{crit,C}$	Critical velocity of $C_D$ reconfiguration	–
Vogel's $E$	Vogel's measure of reconfiguration	–

C. Wilga, J. Heltshe, C. Thornber, Y. Sun, G. Moeser, M. Denny, K. Mach and P. Martone contributed valuable discussions and comments on this manuscript. This work was supported by funds from the Phycological Society of America and the URI Office of the Provost to M.L.B. and from National Science Foundation grant OCE-0082605 to E.C.

### References

- Alben, S., Shelley, M. and Zhang, J. (2002). Drag reduction through self-similar bending of a flexible body. *Nature* **420**, 479-481.
- Alben, S., Shelley, M. and Zhang, J. (2004). How flexibility induces streamlining in a two-dimensional flow. *Phys. Fluids* **16**, 1694-1713.
- Bell, E. C. (1999). Applying flow tank measurements to the surf zone: predicting dislodgment of the Gigartinaceae. *Phycol. Res.* **47**, 159-166.
- Blanchette, C. A. (1997). Size and survival of intertidal plants in response to wave action: a case study with *Fucus gardneri*. *Ecology* **78**, 1563-1578.
- Boller, M. L. and Carrington, E. (2006a). The hydrodynamic effects of shape and size change during reconfiguration of a flexible macroalga. *J. Exp. Biol.* **209**, 1894-1903.
- Boller, M. L. and Carrington, E. (2006b). *In situ* measurements of hydrodynamic forces imposed on *Chondrus crispus* Stackhouse. *J. Exp. Mar. Biol. Ecol.* **337**, 159-170.
- Carrington, E. (1990). Drag and dislodgment of an intertidal macroalga – consequences of morphological variation in *Mastocarpus papillatus* Kutzing. *J. Exp. Mar. Biol. Ecol.* **139**, 185-200.
- Carrington, E., Grace, S. P. and Chopin, T. (2001). Life history phases and the biomechanical properties of the red alga *Chondrus crispus* (Rhodophyta). *J. Phycol.* **37**, 699-704.
- Dayton, P. K. (1973). Dispersion, dispersal, and persistence of annual intertidal alga, *Postelsia palmaeformis* Ruprecht. *Ecology* **54**, 433-438.
- Denny, M. W. (1988). *Biology and Mechanics of the Wave-Swept Environment*. Princeton: Princeton University Press.
- Denny, M. and Gaylord, B. (2002). The mechanics of wave-swept algae. *J. Exp. Biol.* **205**, 1355-1362.
- Denny, M. W., Daniel, T. L. and Koehl, M. A. R. (1985). Mechanical limits to size in wave-swept organisms. *Ecol. Monogr.* **55**, 69-102.
- Dudgeon, S. R. and Johnson, A. S. (1992). Thick vs thin – thallus morphology and tissue mechanics influence differential drag and dislodgment of two codominant seaweeds. *J. Exp. Mar. Biol. Ecol.* **165**, 23-43.
- Garbary, D. J. and DeWreede, R. E. (1988). Life history phases in natural populations of Gigartinaceae (Rhodophyta): quantification using resorcinol. In *Experimental Phycology* (ed. C. S. Lobban, D. J. Chapman and B. P. Kramer), pp. 174-178. Cambridge: Cambridge University Press.
- Gaylord, B. (2000). Biological implications of surf-zone flow complexity. *Limnol. Oceanogr.* **45**, 174-188.
- Gaylord, B. and Denny, M. W. (1997). Flow and flexibility. I. Effects of size, shape and stiffness in determining wave forces on the stipitate kelps *Eisenia arborea* and *Pterygophora californica*. *J. Exp. Biol.* **200**, 3141-3164.
- Gaylord, B., Blanchette, C. A. and Denny, M. W. (1994). Mechanical consequences of size in wave-swept algae. *Ecol. Monogr.* **64**, 287-313.
- Gaylord, B., Hale, B. B. and Denny, M. W. (2001). Consequences of

- transient fluid forces for compliant benthic organisms. *J. Exp. Biol.* **204**, 1347-1360.
- Gere, J. M. and Timoshenko, S. P.** (1984). *Mechanics of Materials*. Monterey, CA: Brooks/Cole Engineering Division.
- Graham, L. E. and Wilcox, L. W.** (2000). *Algae*. Upper Saddle River, NJ: Prentice Hall.
- Hale, B. B.** (2001). Material properties of marine algae and their role in the survival of plants in flow. PhD thesis, Stanford University, USA.
- Harder, D. L., Speck, O., Hurd, C. L. and Speck, T.** (2004). Reconfiguration as a prerequisite for survival in highly unstable flow-dominated habitats. *J. Plant Growth Regul.* **23**, 98-107.
- Harder, D. L., Hurd, C. L. and Speck, T.** (2006). Comparison of mechanical properties of four large, wave-exposed seaweeds. *Am. J. Bot.* **93**, 1426-1432.
- Hoerner, S. F.** (1965). *Fluid-dynamic Drag*. Brick Town, NJ: Published by author.
- Holbrook, N. M., Denny, M. W. and Koehl, M. A. R.** (1991). Intertidal trees – consequences of aggregation on the mechanical and photosynthetic properties of sea-palms *Postelsia palmaeformis* Ruprecht. *J. Exp. Mar. Biol. Ecol.* **146**, 39-67.
- Koehl, M. A. R.** (1984). How do benthic organisms withstand moving water. *Am. Zool.* **24**, 57-70.
- Koehl, M. A. R.** (1986). Mechanical design of spicule-reinforced connective tissues. *Am. Zool.* **26**, A38.
- Koehl, M. A. R.** (1996). When does morphology matter? *Annu. Rev. Ecol. Syst.* **27**, 501-542.
- Koehl, M. A. R. and Alberte, R. S.** (1988). Flow, flapping, and photosynthesis of *Nereocystis luetkeana* – a functional comparison of undulate and flat blade morphologies. *Mar. Biol.* **99**, 435-444.
- Koehl, M. A. R. and Wainwright, S. A.** (1977). Mechanical adaptations of a giant kelp. *Limnol. Oceanogr.* **22**, 1067-1071.
- Padilla, D. K. and Allen, B. J.** (2000). Paradigm lost: reconsidering functional form and group hypotheses in marine ecology. *J. Exp. Mar. Biol. Ecol.* **250**, 207-221.
- Paine, R. T.** (1979). Disaster, catastrophe, and local persistence of the sea palm *Postelsia palmaeformis*. *Science* **205**, 685-687.
- Pratt, M. C. and Johnson, A. S.** (2002). Strength, drag, and dislodgment of two competing intertidal algae from two wave exposures and four seasons. *J. Exp. Mar. Biol. Ecol.* **272**, 71-101.
- Sand-Jensen, K.** (2003). Drag and reconfiguration of freshwater macrophytes. *Freshw. Biol.* **48**, 271-283.
- Stewart, H. L.** (2006). Hydrodynamic consequences of flexural stiffness and buoyancy for seaweeds: a study using physical models. *J. Exp. Biol.* **209**, 2170-2181.
- Underwood, A. J.** (1997). *Experiments in Ecology*. Cambridge: Cambridge University Press.
- Vogel, S.** (1984). Drag and flexibility in sessile organisms. *Am. Zool.* **24**, 37-44.
- Vogel, S.** (1989). Drag and reconfiguration of broad leaves in high winds. *J. Exp. Bot.* **40**, 941-948.
- Vogel, S.** (1994). *Life in Moving Fluids*. Princeton: Princeton University Press.
- Wainwright, S. A., Biggs, W. D., Currey, J. D. and Gosline, J. M.** (1976). *Mechanical Design in Organisms*. London: Edward Arnold.